Application of rubber artificial muscle manipulator as a rehabilitation robot

Toshiro Noritsugu
Okayama University

Toshihiro Tanaka
Okayama University

Application of Rubber Artificial Muscle Manipulator as a Rehabilitation Robot

Toshiro Noritsugu and Toshihiro Tanaka

***Abstract*—The application of a robot to rehabilitation has become a matter of great concern. This paper deals with functional recovery therapy, one important aspect of physical rehabilitation. Single-joint therapy machines have already been achieved. However, for more efficient therapy, multijoint robots are necessary to achieve more realistic motion patterns. This kind of robot must have a high level of safety for humans. A pneumatic actuator may be available for such a robot, because of the compliance of compressed air. A pneumatic rubber artificial muscle manipulator has been applied to construct a therapy robot with two degrees of freedom (DOF). Also, an impedance control strategy is employed to realize various motion modes for the physical therapy modes. Further, for efficient rehabilitation, it is desirable to comprehend the physical condition of the patient. Thus, the mechanical impedance of the human arm is used as an objective evaluation of recovery, and an estimation method is proposed. Experiments show the suitability of the proposed rehabilitation robot system.**

***Index Terms*—Human-friendly robot, impedance control, pneumatic system, rehabilitation robot, rubber artificial muscle.**

I. Introduction

THE number of humans requiring rehabilitation due to fracture of a bone and joint disease caused by traffic accidents and cerebral apoplexy and for functional problems in motion due to advanced age reaches several hundreds of thousands in Japan. Functional recovery therapy of rehabilitation is normally carried out by medical therapists on a person-to-person basis, but automatic equipment has been put to practical use in physical therapy programs that repeat relatively simple operations, such as a continuous passive motion (CPM) machine, a walking training device, or a torque machine used for a single axis [1], [2].

For practical physical therapy, a robot manipulator with multiple degrees of freedom (DOF) is desirable. Since, for the purpose of rehabilitation, it is impossible to distinguish between the robot working space and the human existing space, the robot must provide high levels of safety and flexibility for humans that are not common in general industrial robots. For this function, the robot must be constructionally flexible. However, this kind of robot has not been extensively studied.

In this paper, we use pneumatic rubber artificial muscle actuators to operate a 2-DOF manipulator driven for the functional recovery therapy. Four motion modes for physical therapy are demonstrated using an impedance control system [3], which contains a 2-DOF proportional integral and differential (PID) position control system provided with the inner pressure control loop. This allows the therapy motion modes to be realized in an integrated way. Through experiments of speed control, compliance, and damping control, satisfactory control performance can be obtained.

To execute rehabilitation more efficiently, it is desired that the robot adjust its own impedance parameters according to the physical condition of the patient. For this purpose, the mechanical impedance of the human arm under therapy is used as an objective evaluation index for recovery, and an estimation method based on an adaptive identification technique is proposed. The estimation performance is experimentally investigated. The estimation will be simultaneously carried out with the functional recovery therapy by using the same manipulator.

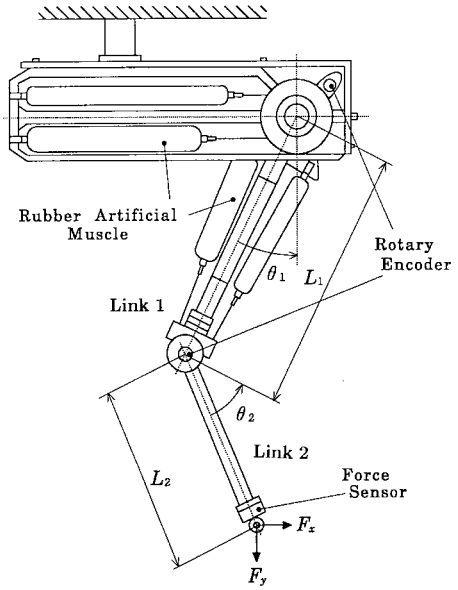

Fig. 1. Rubber artificial muscle manipulator.

II. Construction of Robot System

A. Experimental Manipulator

This paper deals with a 2-DOF manipulator for the functional recovery therapy of a human arm. Fig. 1 shows the experimental rubber artificial muscle manipulator extending

Manuscript received February 18, 1997; revised August 23, 1997. Recommended by Guest Editor H. Kobayashi.

The authors are with the Department of Systems Engineering, Faculty of Engineering, Okayama University, Okayama, 700 Japan (e-mail: toshiro@sys.okayama-u.ac.jp).

Publisher Item Identifier S 1083-4435(97)09029-7.

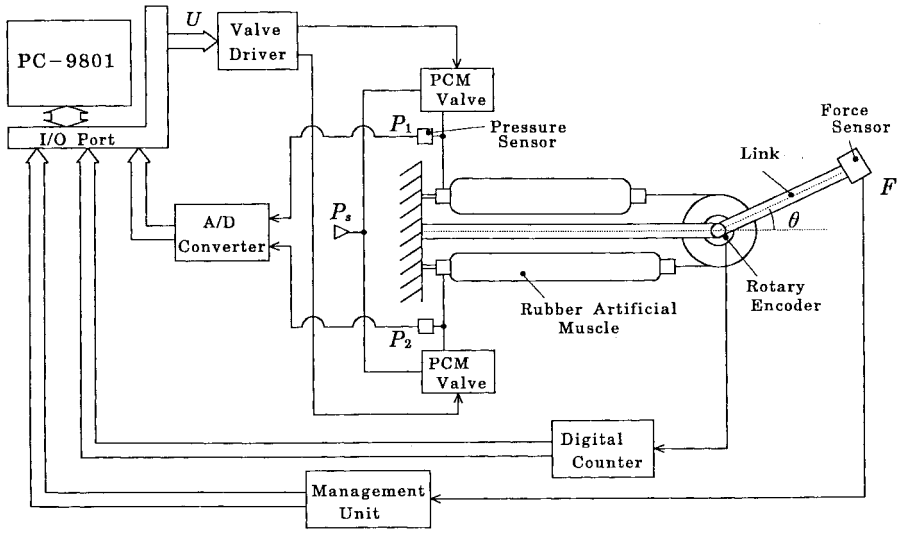

Fig. 2. Control system for each 1-DOF joint.

down against the force of gravity; it has a link length of $L_1 = 410$ mm and $L_2 = 385$ mm, similar to the human arm. Each joint is driven by two actuators in an antagonist pair. Each actuator comprises two rubber artificial muscles (Rubbertuator RUB-835S (link 1), RUB-825S (link 2) from Bridgestone Company, Japan) to strengthen the generated torque. Joint angles θ_1 and θ_2 are detected using rotary encoders with the resolution of 0009° and 0.011°, respectively. A six-axes-type force sensor is equipped at the end of link 2 to measure horizontal (x direction) and vertical (y direction) subjected forces F_x, F_y with the resolution of 0.21 and 0.11 N, respectively.

Fig. 2 shows the experimental control system for each joint. The actuator is driven by a 7-b pulse code modulation (PCM) digital control valve, which has been developed to operate as an equivalent proportional valve with only ON–OFF valves [4]. Each control valve is built using seven three-port ON–OFF solenoid valves and flow restrictors, as shown in Fig. MP3. The effective cross-sectional area S_i (i is from 0 to 6) of the combination of valve and restrictor is designed to satisfy the following relation:

$$S_0 : S_1 : S_2 : S_3 : S_4 : S_5 : S_6 = 2^0 : 2^1 : 2^2 : 2^3 : 2^4 : 2^5 : 2^6. \quad (1)$$

The 7-b PCM valve can adjust the actuator pressure to 2^7 steps. The supply pressure P_s is 550 kPa. Actuator pressures are detected with the resolution of 0.29 kPa.

The control input U is an integer of $0 \leq U \leq 127$, $U = 0$ corresponding to wholly exhausting and $U = 127$ to wholly supplying. The controller to generate U is constructed in the digital personal computer using a C-language program.

B. Pressure Control System

The control performance of rubber artificial muscle actuator depends on the characteristic of pressure response; therefore, the pressure should be controlled as rapidly and accurately as possible. Air compressibility is effective in obtaining flexibility, but causes a control delay in the pressure response.

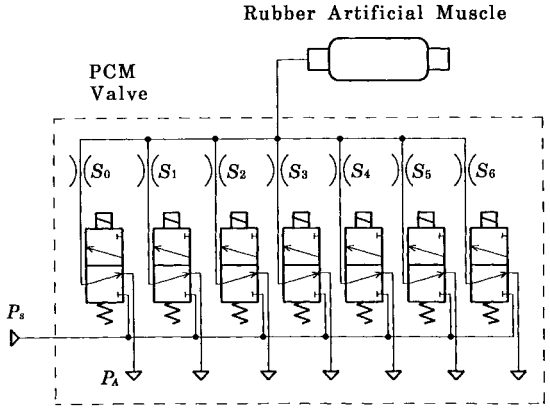

Fig. 3. 7-b PCM digital control valve.

To construct a pneumatic system, the compensation of the pressure control delay is an important issue. A pressure feedback control may be one effective approach.

For the purpose of obtaining a rapid and stable pressure response, the pressure control system shown in Fig. 4 is constructed for two antagonist pairs of muscles to drive links 1 and 2. The desired pressures $\boldsymbol{P}_{rf} = [P_{rf1}, P_{rf2}]^T$ and $\boldsymbol{P}_{re} = [P_{re1}, P_{re2}]^T$ are generated by the following equation:

$$\boldsymbol{P}_{rf} = \boldsymbol{P}_0 + \boldsymbol{dP}, \boldsymbol{P}_{re} = \boldsymbol{P}_0 - \boldsymbol{dP} \quad (2)$$

where $\boldsymbol{P}_0 = [P_{01}, P_{02}]^T$ is the initial reference pressure, and $\boldsymbol{dP} = [dP_1, dP_2]^T$ is the control pressure input from the preceding controller. Subscripts f and e denote quantities of flexor and extensor side, respectively. Also, 1 and 2 correspond to links 1 and 2.

$\boldsymbol{U}_{0f}$ and $\boldsymbol{U}_{0e}$ are control inputs into PCM valves to generate $\boldsymbol{P}_0$, determined from the static characteristic of the valve. In order to achieve the desired pressures, the actuator pressure is controlled by a feedback proportional integral (PI) controller. The relation between the control input $\boldsymbol{U}_f$ into the PCM valve and the resultant pressure $\boldsymbol{P}_f$ is nonlinear. The relation between $\boldsymbol{U}_e$ and $\boldsymbol{P}_e$ is the same. The nonlinearity is

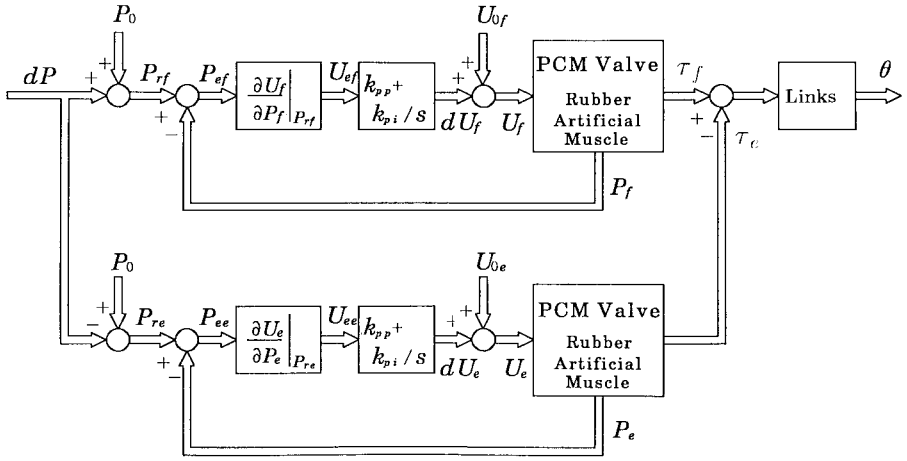

Fig. 4. Pressure control system for antagonist pair of muscles.

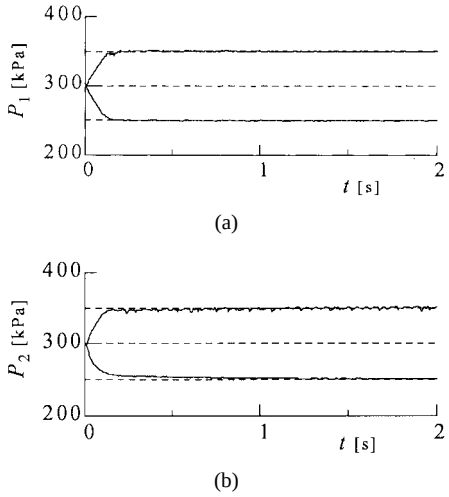

Fig. 5. Characteristics of pressure response. (a) Link 1. (b) Link 2.

compensated by using slopes $\partial \boldsymbol{U}_f/\partial \boldsymbol{P}_f$ and $\partial \boldsymbol{U}_e/\partial \boldsymbol{P}_e$ evaluated at the desired pressure value on the static characteristic approximation curve measured beforehand. $\boldsymbol{P}_{ef}$ and $\boldsymbol{P}_{ee}$ are pressure control errors. $\boldsymbol{U}_{ef}$ and $\boldsymbol{U}_{ee}$ are corresponding control errors, from which PI controllers generate $\boldsymbol{dU}_f$ and $\boldsymbol{dU}_e$. The control gains $\boldsymbol{k}_{pp}$ and $\boldsymbol{k}_{pi}$ are adjusted to obtain the desired pressure response.

The output pressures $\boldsymbol{P}_f$ and $\boldsymbol{P}_e$ generate longitudinal forces in each actuator, which produce torques $\boldsymbol{\tau}_f$ and $\boldsymbol{\tau}_e$, respectively. The difference $\boldsymbol{\tau}_f - \boldsymbol{\tau}_e$ drives the link and robot.

Fig. 5 shows the step responses when $P_{01} = P_{02} = 300$ kPa, $dP_1 = dP_2 = 50$ kPa. Fig. 5(a) and (b) are the results of links 1 and 2, respectively. The control gains $\boldsymbol{k}_{pp}$ and $\boldsymbol{k}_{pi}$ have been determined by the trial-and-error method in the experiments. The pressure can respond with the time constant of about 0.1 s, which may be enough fast for rehabilitation.

C. Impedance Control System

In the x–y coordinate shown in Fig. 6, the position of the end of link 2 $\boldsymbol{X} = [x, y]^T$ and the contact force $\boldsymbol{F} = [F_x, F_y]^T$ are controlled to satisfy the following relation:

$$\boldsymbol{F} = \boldsymbol{B}(\dot{\boldsymbol{X}}_d - \dot{\boldsymbol{X}}) + \boldsymbol{K}(\boldsymbol{X}_d - \boldsymbol{X}) \tag{3}$$

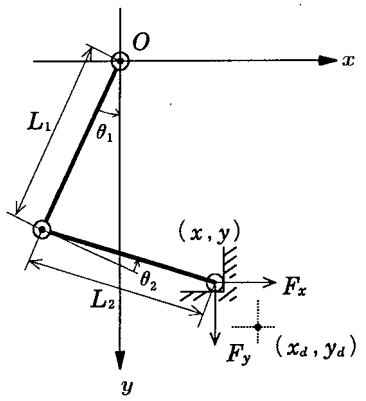

Fig. 6. Model of manipulator contacting with object.

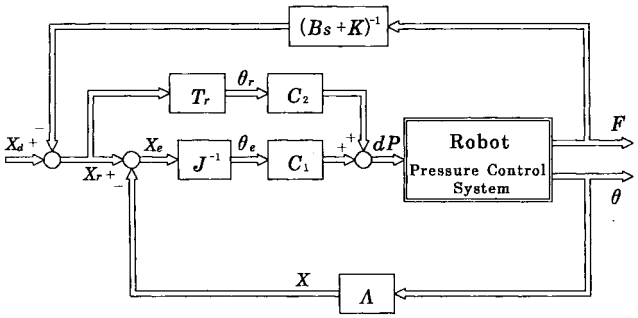

Fig. 7. Constructed impedance control system.

where $\boldsymbol{X}_d$ is the hypothetical desired position. $\boldsymbol{B} = \mathrm{diag}(b_x, b_y)$ and $\boldsymbol{K} = \mathrm{diag}(k_x, k_y)$ denote the desired damping and stiffness, respectively. Fig. 7 shows the position-based impedance control system constructed in this paper, where practically measured forces $\boldsymbol{F}$ and joint angles $\boldsymbol{\theta}$ are indicated as output variables. If the inner position control loop ideally operated to make $\boldsymbol{X} = \boldsymbol{X}_r$, the desired impedance described by (3) could be realized [5]. Naturally, when $\boldsymbol{X}$ cannot exactly follow $\boldsymbol{X}_r$, the resultant impedance does not completely agree with (3). The inner position control loop should be designed to operate as ideally as possible in the necessary frequency range.

The rubber artificial muscle actuator has so little damping that a satisfactory continuous trajectory control is not easy

to obtain with the usual feedback control. Instead, a 2-DOF control system with feedforward compensation is constructed. $\boldsymbol{C}_1$ and $\boldsymbol{C}_2$ are PI and proportional integral (PD) controllers, respectively. Both the disturbance suppression characteristic and the tracking property can be independently specified by $\boldsymbol{C}_1$ and $\boldsymbol{C}_2$. The proportional gain of $\boldsymbol{C}_2$ is determined from the relation between pressure and displacement of the rubber artificial muscle actuator measured, considering the gravity effect. Λ denotes the inverse kinematics transforming the joint angle $\boldsymbol{\theta} = [\theta_1, \theta_2]^T$ to the Cartesian position $\boldsymbol{X}$. $\boldsymbol{J}$ is the Jacobian. $\boldsymbol{T}_r$ denotes the following transformation:

$$\boldsymbol{\theta}_r(t+T) = \boldsymbol{\theta}_r(t) + \boldsymbol{J}^{-1}[\boldsymbol{X}_r(t+T) - \boldsymbol{X}_r(t)] \qquad (4)$$

where T is a sampling period. The initial desired joint angle $\theta_r(0)$ is calculated to give the initial desired position $\boldsymbol{X}_r(0)$.

This impedance control system operates as a position control system when not contacting ($\boldsymbol{F} = 0$). The smaller the desired stiffness $\boldsymbol{K}$ becomes, the faster the control system can respond, but lesser is the stability margin. A large desired damping $\boldsymbol{B}$ will improve the stability.

D. Application to Functional Recovery Therapy

There are many kinds of therapy for functional recovery in rehabilitation. Such therapy is performed by the therapist who adjusts the load force and speed to meet the requirements of a patient, but there are many kinds of therapy that can be performed by machines, such as the application of a certain load to the human arm or repetition of joint bending and stretching at a low speed. The following four motion modes have been defined for physical therapy by the robot manipulator.

1) *Isometric Mode:* The robot arm receives the force from the patient at the stationary state. This mode can be achieved by means of the extremely high impedance and the constant $\boldsymbol{X}_d$.
2) *Isokinetic Mode P (Patient Passive):* The robot arm operates at the constant speed, regardless of the force from the patient. This mode is used for reinforcement therapy or extension of the movable region of the human muscle, which can be achieved by setting $\boldsymbol{X}_d$ as a ramp signal. The safety of the patient having only small muscular strength is achieved by setting a low desired impedance.
3) *Isokinetic Mode A (Patient Active):* The patient tries to move the arm at the constant speed. The reaction force is proportional to the arm speed. This mode can be obtained from the damping control specified by $\boldsymbol{B}$, where $\boldsymbol{X}_d$ is constant and $\boldsymbol{K} = \boldsymbol{0}$.
4) *Isotonic Mode:* The arm gives the patient the constant force to increase the muscular strength. This mode can be realized by setting $\boldsymbol{K}$ and $\boldsymbol{dX} = \boldsymbol{X}_d - \boldsymbol{X}$ at constant values.

Setting up $\boldsymbol{K}$, $\boldsymbol{B}$, and $\boldsymbol{X}_d$ by the above-described methods enables the four therapy modes to be implemented.

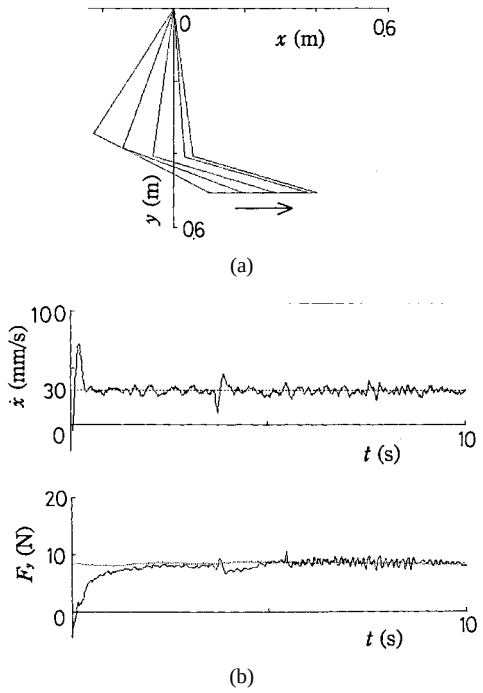

Fig. 8. Contacting trajectory control. (a) Arm configuration in 3-s increments. (b) Speed and contact force.

III. Results of Recovery Therapy Motion

A. Compliance Control

A standard compliance control has been executed to examine the fundamental motion control performance of the experimental robot. Fig. 8 shows the response of contacting trajectory control, where $k_x = k_y = 1000$ N/m, $\boldsymbol{B} = \boldsymbol{0}$. The arm contacts with the object wall at $y = 0.53$ m. The desired speed in the x direction $\dot{x}_d = 30$ mm/s and $y_d = 0.54$ m. The desired force F_y, shown by a dotted line calculated by (3), does not become a completely straight line, due to the deflection of robot links. When the desired damping $\boldsymbol{B}$ is large, the stability margin of the control system becomes larger, so that the smaller stiffness can be realized. It has been confirmed that when $\boldsymbol{B} = \boldsymbol{0}$, a stiffness larger than 500 N·s/m can be stably achieved in the experimental robot system. The parameters of controllers $\boldsymbol{C}_1$ and $\boldsymbol{C}_2$ have been adjusted by the trial-and-error method, details of which can be found in [6]. Both the desired compliance and tracking speed can be realized with satisfactory accuracy.

B. Motion Mode for Recovery Therapy

Fig. 9 shows an experimental view using the therapy robot. Assuming therapy by means of the almost horizontally straight line trajectory, the human puts recovery load on the end effector, as shown in Fig. 9. Each motion mode is achieved in only the x direction. In the y direction, the usual compliance control is executed. Since the isometric therapy mode does not require any control, it is not discussed in this section.

1) Isokinetic Mode P: Fig. 10 shows the response being subjected to the intentional load force by the human, which also demonstrates the speed control performance of the robot

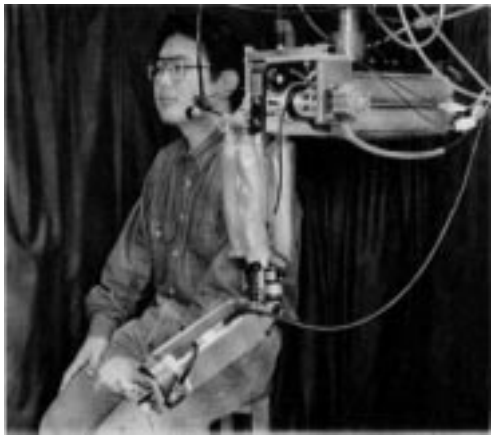

Fig. 9. Overview of experimental therapy robot.

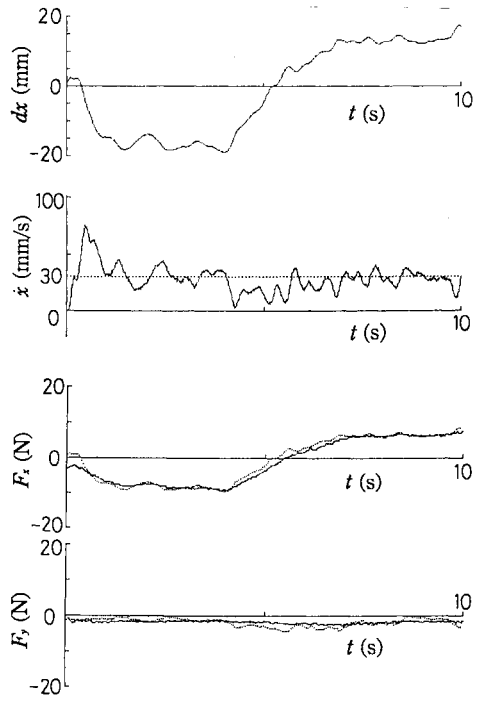

Fig. 10. Isokinetic motion mode P.

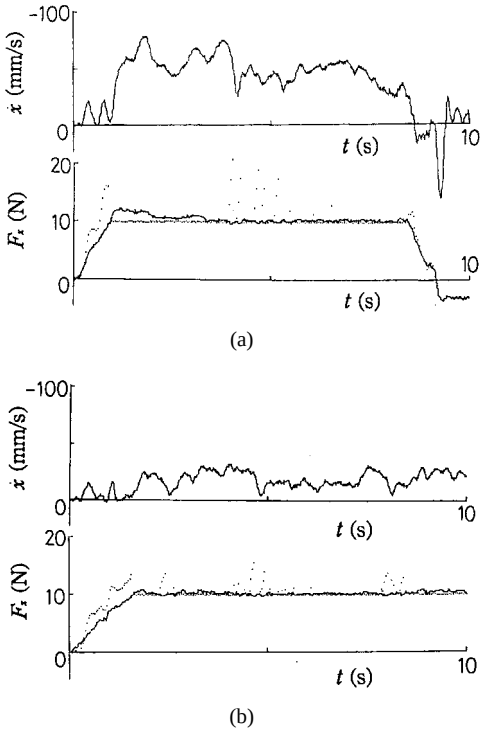

Fig. 11. Isotonic motion mode. (a) Fast motion. (b) Slow motion.

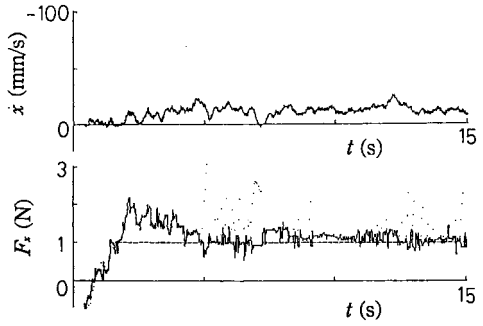

Fig. 12. Isotonic motion mode for small force.

manipulator, where, $k_x = 500$ N/m, $k_y = 1000$ N/m, $\boldsymbol{B} = \boldsymbol{0}$, and $\dot{x}_d = 30$ mm/s. When $dx = x_d - x$ is negative, the robot manipulator restrains the motion of the human arm in the x direction. On the contrary, when dx is positive, the robot manipulator pulls the human arm in the x direction. In either case, the reaction force agrees with the desired value (shown by dotted lines) calculated by (3), in spite of the direction of force. The speed control error increases when the load force changes, because of the response delay of the robot. However, when the change of load force is not so rapid, the robot can move at the nearly desired average speed. It can be considered that such control performance is sufficient for the isokinetic mode P. In the y direction, the force from the weight of the human hand and arm appears.

2) Isotonic Mode: Fig. 11 shows the force response when the human moves the arm at various speeds, where $k_x = 2000$ N/m, $k_y = 1000$ N/m, $\boldsymbol{B} = \boldsymbol{0}$, and $dx = 0.005$ m, so that the desired force in x direction is 10 N. Before the force reaches the desired force $k_x dx$, indicated by dotted line, the usual compliance control is executed based on fixed x_d to shorten the rising time of the force response. When the force exceeds the desired value, x_d is changed to keep $dx = 0.005$ m. At the moment the force decreases under the desired value, x_d is fixed at that momentary value. The value of dx can be known as the ratio of the desired force to $k_x = 2000$ N/m.

Fig. 12 shows the response for the small desired force of 1 N, where $k_x = 1000$ N/m and $dx = 0.001$ m. After the initial transient region, the controlled force approaches the desired force. The relatively small force control can be satisfactorily achieved.

3) Isokinetic Mode A: Fig. 13 shows the response of damping control to realize the isokinetic mode A, where $b_x = 300$ N·s/m, $k_y = 1000$ N/m, $k_x = b_y = 0$, and the robot manipulator is moved by the human arm. The force satisfactorily coincides with the desired force ($-b_x \dot{x}$) shown by dotted lines over the wide range of arm speed. Fig. 14

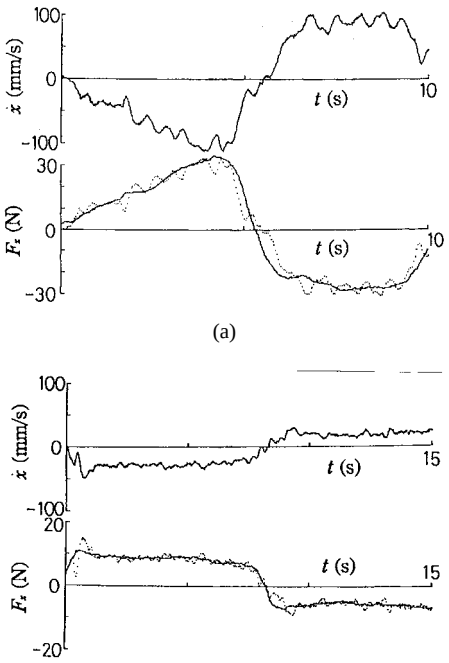

Fig. 13. Isokinetic motion mode A. (a) Fast motion. (b) Slow motion.

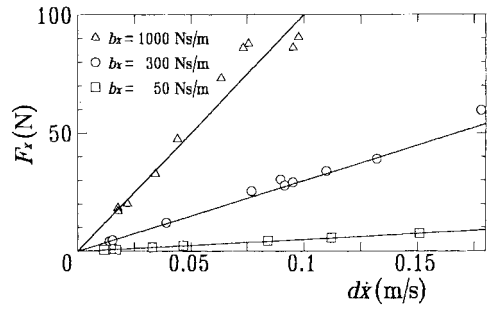

Fig. 14. Accuracy of damping control.

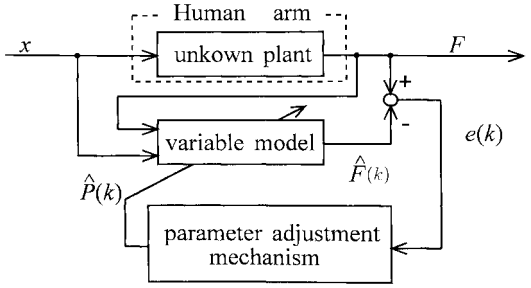

Fig. 15. Parameter estimation system.

shows the accuracy of the damping control for some desired damping values b_x. The figure illustrates the possibility of accurate damping control to execute the recovery therapy of isokinetic motion mode A.

IV. Estimation of Human Condition

An efficient rehabilitation requires one to estimate the physical recovery condition of patients by using an appropriate evaluation index. In this paper, the mechanical impedance of the human arm is proposed as an objective evaluation index [7], [8]. The rubber artificial muscle manipulator is used for the purpose of simultaneously performing the recovery therapy and the estimation of arm impedance to measure the physical recovery condition. In the system shown in Fig. 9, the manipulator oscillates the human arm at the end of link 2 in the vertical x–y plane. The human arm is modeled by a mechanical impedance model, of which unknown impedance parameters described in the x–y coordinate are estimated by means of an adaptive identification scheme.

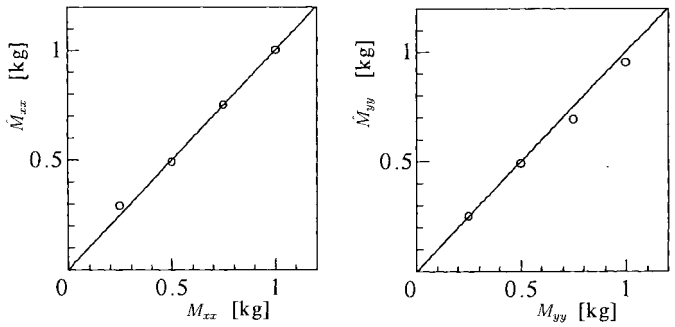

Fig. 16. Estimation of known mass.

A. Human Mechanical Impedance Model

A human arm is modeled as a 2-DOF link mechanism. Its mechanical impedance model is described as follows, wherein the parameters are estimated:

$$\boldsymbol{F}_h = \boldsymbol{M}\ddot{\boldsymbol{X}} + \boldsymbol{B}\dot{\boldsymbol{X}} + \boldsymbol{K}\boldsymbol{X} \tag{5}$$

where

$$\boldsymbol{M} = \begin{bmatrix} M_{xx} & M_{xy} \\ M_{yx} & M_{yy} \end{bmatrix}, \qquad \boldsymbol{B} = \begin{bmatrix} B_{xx} & B_{xy} \\ B_{yx} & B_{yy} \end{bmatrix}$$
$$\boldsymbol{K} = \begin{bmatrix} K_{xx} & K_{xy} \\ K_{yx} & K_{yy} \end{bmatrix}$$

are inertia, damping, and stiffness matrices, respectively, described in the x–y coordinate. $\boldsymbol{F}_h = [F_{hx}, F_{hy}]^T$ is a passive reaction force from the human arm. Other force not included in $\boldsymbol{F}_h$ is considered as a disturbance in the model. The impedance model to be identified is given by

$$\boldsymbol{F} = \boldsymbol{M}\ddot{\boldsymbol{X}} + \boldsymbol{B}\dot{\boldsymbol{X}} + \boldsymbol{K}\boldsymbol{X} + \boldsymbol{F}_a = \boldsymbol{P}\boldsymbol{\zeta} \tag{6}$$

where $\boldsymbol{F} = [F_x, F_y]^T$ is the output from the unknown plant (human arm), detected with the force sensor. $\boldsymbol{F}_a = [F_{ax}, F_{ay}]^T$ corresponds to the disturbance, including an active force intentionally generated by the human. F_{ay} also includes the gravity term.

$\boldsymbol{P} = [\boldsymbol{P}_x, \boldsymbol{P}_y]^T$ and $\boldsymbol{\zeta}$ are a parameter matrix and a state variable vector, respectively, shown as

$$\boldsymbol{P}_x = [M_{xx}\, M_{xy}\, B_{xx}\, B_{xy}\, K_{xx}\, K_{xy}\, F_{ax}] \tag{7}$$
$$\boldsymbol{P}_y = [M_{yx}\, M_{yy}\, B_{yx}\, B_{yy}\, K_{yx}\, K_{yy}\, F_{ay}] \tag{8}$$
$$\boldsymbol{\zeta}^T = [\ddot{x}\, \ddot{y}\, \dot{x}\, \dot{y}\, x\, y\, 1]. \tag{9}$$

The mechanical impedance parameters are estimated as components of parameter vectors $\boldsymbol{P}_x$ and $\boldsymbol{P}_y$.

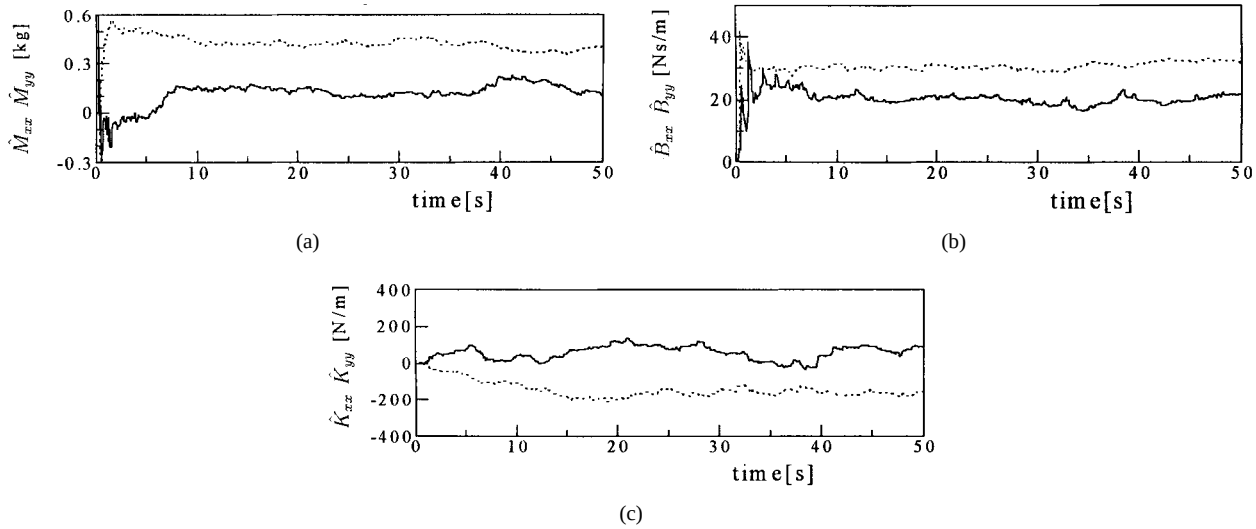

Fig. 17. Estimated human impedance parameters in relaxed condition. (a) Mass. (b) Damping. (c) Stiffness.

B. Parameter Estimation Algorithm

Fig. 15 shows a parameter estimation system. The usual discrete-time adaptive identification method is used. For the unknown plant model of (6), the identification discrete-time model is defined as

$$\hat{\boldsymbol{F}}(k) = \hat{\boldsymbol{P}}(k)\boldsymbol{\zeta}(k) \tag{10}$$

where $\hat{\boldsymbol{P}}(k)$ denotes the parameter matrix to be estimated, and k denotes the discrete value at the time kT. For the error equation

$$\boldsymbol{e}(k) = [\boldsymbol{P} - \hat{\boldsymbol{P}}(k)]\boldsymbol{\zeta}(k) \tag{11}$$

the following parameter adjustment algorithm is used:

$$\hat{\boldsymbol{P}}(k) = \hat{\boldsymbol{P}}(k-1) + \boldsymbol{\Gamma}(k-1)\boldsymbol{\zeta}(k)\boldsymbol{e}(k) \tag{12}$$

$$\boldsymbol{\Gamma}(k) = \frac{1}{\lambda_1(k)} \cdot \left[\boldsymbol{\Gamma}(k-1) - \frac{\lambda_2(k)\boldsymbol{\Gamma}(k-1)\boldsymbol{\zeta}(k)\boldsymbol{\zeta}^T(k)\boldsymbol{\Gamma}(k-1)}{\lambda_1(k) + \lambda_2(k)\boldsymbol{\zeta}^T(k)\boldsymbol{\Gamma}(k-1)\boldsymbol{\zeta}(k)}\right] \tag{13}$$

where $0 < \lambda_1(k) \leq 1$, $0 \leq \lambda_2(k) < 2$, and $\boldsymbol{\Gamma}(0) > 0$. There are some methods to determine $\lambda_1(k)$ and $\lambda_2(k)$. This paper employs a constant-trace algorithm which determines $\lambda_1(k)$ and $\lambda_2(k)$, so that the trace of $\boldsymbol{\Gamma}(k)$ becomes constant. The value of the trace should be chosen for the parameter adjustment to be stable. When stable, $\hat{\boldsymbol{P}}(k)$ can approach the true value $\boldsymbol{P}$.

C. Results of Estimation

1) Generation of Exciting Displacement: The excitation signal should contain as many kinds of frequency components as possible to improve the estimation performance. It has been confirmed that the experimental robot manipulator shown in Fig. 9 can effectively excite the human arm from 0 to about 3 Hz in both x and y directions. In experiments, to generate the exciting displacement, the random fluctuations with the maximum amplitude of 30 mm are added to the desired position $\boldsymbol{X}_d$ in Fig. 7. Now, the force feedback loop is cut off to execute the usual position control.

2) Estimation Performance: A known mass is attached to the end of the manipulator, the vaue of which is estimated to examine the estimation performance. $\ddot{x}$, $\ddot{y}$, $\dot{x}$, and $\dot{y}$, required in the estimation algorithm, are approximated by the differentiation of x and y, respectively. Fig. 16 shows estimated mass $\hat{M}_{xx}$ and $\hat{M}_{yy}$ compared with the true value, indicated by a solid line. Estimated values coincide well with true values, confirming the availability of the proposed estimation method.

3) Human Impedance Parameter: The above random fluctuations are imposed on the human arm, which keeps an attitude similarly expressed by the configuration when $\theta_1 = \theta_2 = 0$ in Fig. 6, i.e., upper arm and forearm take vertical and horizontal attitudes, respectively. Fig. 17 shows the estimated parameters when the human arm relaxes as completely as possible. In Fig. 18, the human arm is consciously strained. Solid lines and dotted lines indicate estimated values in x and y directions, respectively. Every parameter converges to a certain estimated value. Concerning the estimated values of mass and damping, there is no significant difference between the results in two cases. However, a large difference can be recognized in the stiffness $\hat{K}_{xx}$. The estimated stiffness $\hat{K}_{xx}$ becomes very large in the strained condition. This agrees well with our understanding.

Fig. 19 shows the result when the human intentionally applies force in the positive x and y directions, 15 s after the start of estimation. Solid and dotted lines indicate the estimated values of F_{ax} and F_{ay}, respectively. The result confirms the validity of the term of $\boldsymbol{F}_a$ in the impedance model of (6). Fig. 20 shows estimated intentional force $\hat{F}_{ay}$ and stiffness $\hat{K}_{yy}$ when the human applies intentional force in the positive y direction at about 33 s. The estimated values of mass and damping have remained almost constant. The result agrees with the fact that the human arm becomes hard when it generates the large force.

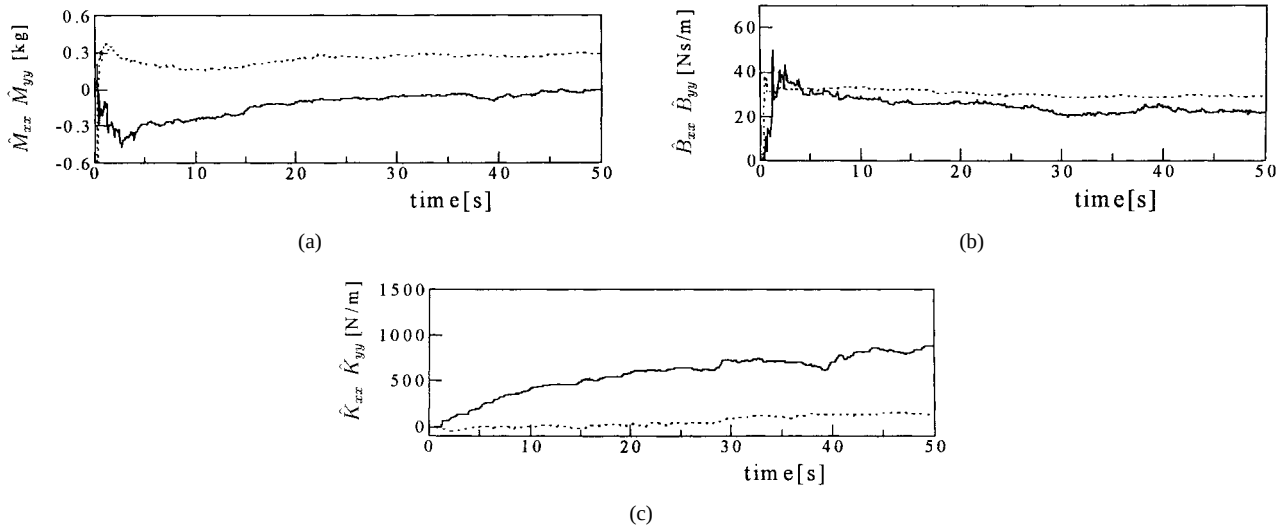

Fig. 18. Estimated human impedance parameters in strained condition. (a) Mass. (b) Damping. (c) Stiffness.

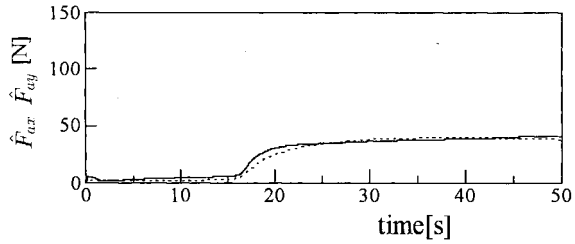

Fig. 19. Estimated intentional force applied by human.

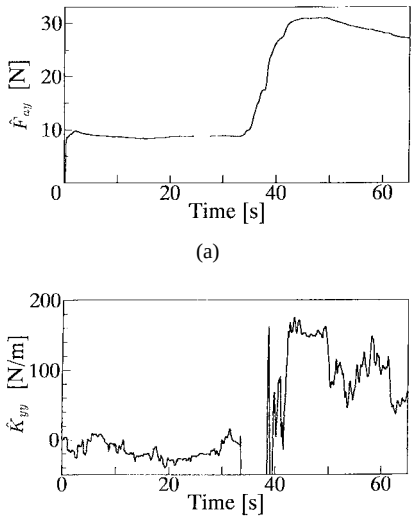

Fig. 20. Increase of stiffness accompanied with intentional force. (a) Intentional force. (b) Stiffness.

Although further work is needed to discuss the accuracy of estimation, it is confirmed that at least the estimated stiffness can sensitively reflect the physical condition of the human arm. The estimated stiffness has the possibility of being used as an objective evaluation index for the recovery condition. However, it is not currently easy for the authors to medically describe the relation between the stiffness and the recovery condition. Such a medical description will be the object of future work.

V. Conclusion

The rehabilitation robot does not require highly accurate position or force control, but, rather, the safety and flexibility for the patient. From such a point of view, this paper has applied the rubber artificial muscle actuator to a therapy robot for the physical functional recovery of the human arm. We have proposed a unified control approach to realize important motion modes for the demonstrated recovery therapy, based on the impedance control strategy. The proposed control approach has been effective. Also, the availability of this actuator to the rehabilitation robot has been confirmed.

Further, an estimation method of the human arm parameters has been proposed for the purpose of evaluating the recovery physical condition of the human arm, which estimates the mechanical impedance of the human arm by means of an adaptive identification method. In experiments, the influence of the physical condition of the human arm has not been significantly recognized in estimated mass and damping, but the estimated stiffness can sensitively reflect the physical condition of the human arm. The estimated stiffness may be available as an evaluation index for physical recovery.

The integration between the recovery therapy and the estimation will comprise important future work, where the mechanical impedance, especially stiffness, may be used as a common significant parameter.

Acknowledgment

The authors would like to acknowledge Bridgestone Corporation, Japan, for providing an experimental rubber artificial muscle manipulator and T. Yamanaka, Bridgestone Corporation, for his contributions to this research project. The authors are also grateful to F. Ando for his important contribution to this study, when he was a master course student.

References

[1] Y. Doi, "Exercise apparatus for restoration of function," *J. Soc. Biomech.*, vol. 17, no. 2, pp. 99–105, 1993.

[2] M. Fujie *et al.*, "Improvement of walking rehabilitation system for elderly," in *Proc. IEEE Int. Conf. Robotics and Automation,* 1995, vol. WS-3, pp. 32–39.
[3] N. Hogan, "Stable execution of contact tasks using impedance control," in *Proc. IEEE Int. Conf. Robotics and Automation,* 1987, pp. 1047–1054.
[4] T. Noritsugu and T. Wada, "Adaptive variable structure control of pneumatically actuated robot," in *Proc. 1st JHPS Int. Symp. Fluid Power,* 1989, pp. 591–598.
[5] D. A. Lawrence, "Impedance control stability properties in common implementation," in *Proc. IEEE Int. Conf. Robotics and Automation,* 1988, pp. 1185–1190.
[6] T. Noritsugu, F. Ando, and T. Yamanaka, "Rehabilitation robot using rubber artificial muscle (1st Report: Realization of exercise motion mode with impedance control," *J. Robot. Soc. Jpn.*, vol. 13, no. 2, pp. 141–148, 1995.
[7] D. J. Bennet, J. M. Hollerbach, Y. Xu, and I. W. Hunter, "Time varying stiffness of human elbow joint during cyclic voluntary movement," *Exp. Brain Res.,* vol. 88, pp. 433–442, 1992.
[8] T. Tsuji, P. Morasso, K. Goto, and K. Ito, "Human hand impedance characteristics during maintained posture in multi-joint arm movements," *Biol. Cybern.,* vol. 72, pp. 476–485, 1995.

Toshiro Noritsugu received the B.E. and M.E. degrees from Okayama University, Okayama, Japan, in 1972 and 1974, respectively, and the Dr. Eng. degree from Kyoto University, Kyoto, Japan, in 1982.

From 1974 to 1985, he was with the Department of Mechanical Engineering, Tsuyama National College of Technology, Tsuyama, Japan. In 1986, he joined the Department of Mechanical Engineering, Faculty of Engineering, Okayama University, as an Associate Professor. He became a Professor in 1991. Since 1996, he has been a Professor with the Department of Systems Engineering. His current research interests are pneumatic servo, development of soft actuator, human-friendly robotics, active vibration control, and intelligent control of mechanical systems.

Dr. Noritsugu is a member of the Japan Society of Mechanical Engineers, Japan Hydraulic and Pneumatic Society, Society of Instrument and Control Engineers, Robotics Society of Japan, Institute of Systems, Control, and Information Engineers, Society of Biomechanisms, and Japan Society for Precision Engineering.

Toshihiro Tanaka received the B.E. and M.E. degrees from Okayama University, Okayama, Japan, in 1995 and 1997, respectively.

Since 1997, he has been with Nozaki Printing Corporation, Kyoto, Japan. His interests have included the application of a rubber artificial muscle manipulator to a human-friendly robot.

Mr. Tanaka is a member of the Japan Hydraulics and Pneumatics Society and the Robotics Society of Japan.